PROCEEDINGS OF SCIENCE

Neutron Star Radii, Core-collapse Supernovae, and the Equation of State of Dense Matter

Andrew W. Steiner*
Institute for Nuclear Theory,
University of Washington, Seattle, WA 98195
E-mail: steiner3@uw.edu

Tobias Fischer
GSI, Helmholtzzentrum für Schwerionenforschung GmbH,
Planckstraße 1, 64291 Darmstadt, Germany
Technische Universität Darmstadt Magdalenenstraße 12, 64289 Darmstadt, Germany
Email: t.fischer@gsi.de

Stefano Gandolfi
Theoretical Division,
Los Alamos National Laboratory, Los Alamos, NM 87545
E-mail: stefano@lanl.gov

Matthias Hempel
Department of Physics,
University of Basel, Klingelbergstr. 82, 4056 Basel, Switzerland
Email: matthias.hempel@unibas.ch

Neutron star mass and radius measurements are becoming sufficiently accurate as to offer astrophysical constraints on the properties of neutron-rich matter near the nuclear saturation density. Current observations, which imply that the radius of a 1.4 solar mass neutron star lies between 10.4 and 12.9 km (95% confidence), also imply that $43 < L < 67$ MeV, where L is a parameter describing the slope of the nuclear symmetry energy and that the neutron skin thickness in lead is relatively small.

These advances in our understanding of dense matter also imply that some equation of state (EOS) tables commonly employed in simulations of core-collapse supernovae are likely incorrect because they generate neutron star radii outside the range suggested by observations. Two new supernova EOS tables (SFHo and SFHx) have been constructed from interactions which reproduce the binding energies and charge radii of heavy nuclei and also match the constraints on the EOS provided by neutron star mass and radius observations.

XII International Symposium on Nuclei in the Cosmos,
August 5-12, 2012
Cairns, Australia

*Speaker.

PoS(NIC XII)038

1. Introduction

To a good approximation, all neutron star mass and radius measurements should lie on one universal mass-versus-radius (M−R) curve. Unlike planets, which have varying compositions and thus varying radii for a fixed mass [1], neutron stars are believed to be nearly compositionally uniform because neutron star matter is driven to its ground state [2]. Rotation [3] and magnetic fields [4] modify this basic picture by about 10%, but this uncertainty is well within our current ability to measure neutron star properties.

The Schwarzchild metric, which describes the structure of a static, non-rotating, non-magnetic, self-gravitating object provides the form of Einstein's field equations which are relevant for neutron stars, the Tolman-Oppenheimer-Volkov equation. This equation naturally provides a one-to-one correspondence between the M−R curve and the pressure as a function of the total energy density, $P(\varepsilon)$, i.e. the (zero-temperature) EOS of dense matter.

The pressure of dense matter is determined principally by the amount of attraction or repulsion between the relevant degrees of freedom. For matter near the nuclear saturation density of 2.7 $\times$ 10^{14} g/cm^3, the EOS is determined by the amount of attraction or repulsion present in two- and three-nucleon forces (higher-body forces are likely not relevant until higher densities).

The current challenge is to use astronomical observations of neutron stars to constrain the EOS of dense matter, and to deduce the nature of three-body nucleon-nucleon forces near the nuclear saturation density, and to extract information on the symmetry energy.

2. Progress in Radius Measurements

As recently as 2007 [2], theoretical models of M−R curves covered a large parameter space, with radii anywhere between 8 and 15 km. This large range of masses and radii, in turn, corresponds to a large range of acceptable equations of state. The status of radius measurements has improved significantly over the past five years, in part because of recent improvements in observations and their interpretation. Low-mass X-ray binaries (LMXBs) are neutron stars which are periodically accreting matter from a low-mass main-sequence companion. Over time, accretion creates a layer of hydrogen and helium which is unstable to a nuclear burning. This instability resolves itself through an X-ray burst, a thermonuclear explosion on the neutron star surface resulting in a 10-100 second long burst of X-rays. There are two types of LMXBs which have proven important for neutron star mass and radius measurements: (i) quiescent LMXBs, i.e. LMXBs which are not currently accreting [5–7] and (ii) LMXBs which exhibit bursts which are sufficiently strong as to propel the photosphere outwards, so-called photospheric radius expansion (PRE) bursts [8–11]. When these objects happen to have distance measurements which are available, either because the LMXB is in a globular cluster or because of some other association, these two types of LMXBs can be used to infer the neutron star radius (and sometimes also the mass).

Another important step in constraining theoretical models [12], is the observation that determining the EOS from mass and radius observations is a *statistical* problem in addition to a nuclear astrophysics problem. Mass and radius observations will always have some uncertainty, and in order to delineate the EOS of dense matter one must understand how that observational uncertainty translates into an uncertainty in the corresponding constraints on the EOS.

The data analysis is complicated by the fact that this is an underconstrained problem and it is thus difficult to apply the traditional analysis based on an appropriately-defined χ^2. The M−R curve and the EOS both contain an infinite number of degrees of freedom, and the number of mass and radius observations will always be finite. Further complicating the problem: the analysis requires some sort of assumption of the neutron star initial mass function in order to know how to associate the observation of any one object to a theoretical M−R curve. Nevertheless, Bayesian analysis is well-suited to these kinds of underconstrained problems and can naturally incorporate assumptions about the neutron star initial mass function.

One of the critical difficulties of the Bayesian formalism is the presence of the prior probabilities, and one must at least ensure that final results hold for any set of reasonable prior distributions. In an overconstrained system, the frequentist method would typically give results almost independent of the parametrization of the EOS. This independence holds in the Bayesian formalism as well when the likelihood function is strongly peaked and priors which vary only weakly are unimportant by comparison. In an underconstrained system this independence fails for both frequentist and Bayesian methods. The EOS parametrization itself is additional prior information which we must vary to ensure our results are robust. In spite of these difficulties, after having sampled a large enough set of prior distributions, one finds that *even though there are many EOSs which are possible, there are many which are very improbable*. In other words, some theoretical models are very finely-tuned and thus unlikely to be correct.

3. Connection to Nuclear Physics near Saturation

Two- and three-body nucleon-nucleon forces play important roles in determining the physics of nuclei and nuclear matter near the saturation density. While the two-body nucleon-nucleon interaction is well-understood, because of the clear connection to scattering phase shifts and the amount of experimental data, the three-nucleon force is not well understood. Very accurate calculations are restricted to light nuclei up to $A = 12$ [13], where the $T = 1/2$ channel dominates over the $T = 3/2$ channel, and as a result the three-neutron force is particularly uncertain. Quantum Monte Carlo has proven to be an indispensable tool to consistently study light-nuclei and neutron matter within the same framework. This technique allows one to constrain three-nucleon forces from the structure of light-nuclei and the properties of nuclear matter. Recent work [14] has demonstrated a clear correlation, driven by the form of microscopic three-body forces, between the magnitude (S) and the derivative of the nuclear symmetry energy (L).

Neutron star masses and radii probe matter over a range of densities, potentially from 10^{13-15} g/cm^3, and thus one important question is to what extent observations constrain the properties of the nucleon-nucleon interaction near the nuclear saturation density. There is a clear correlation between neutron star radii and the pressure of neutron-rich matter above the saturation density, this correlation begins to degrade at lower densities [15].

4. Connection to Core-Collapse Supernovae

The supernova explosion mechanism is intimately connected with the equation of state of dense matter. When the progenitor runs out of fuel, the loss in electron pressure from electron

captures on heavy nuclei causes the core to collapse. A shock wave forms and the collapse halts when the core reaches the nuclear saturation density, due to the large pressure provided by strong nuclear interactions at high densities. The collapsing core "bounces" back, propelling the shock wave outwards. It eventually stalls, having lost energy to the dissociation of nuclei and neutrino emission associated with the shock propagation across the neutrinospheres. The shock must be revived in order for the explosion to proceed. Although several scenarios have been explored, recent works point to the success of the neutrino-heating mechanism in multidimensional simulations [16–19].

The details of the shock revival are weakly connected to the equation of state of dense matter, since neutrino heating is mostly important at the lower densities behind the bounce shock. Nevertheless, an indirect impact of the high-density equation of state can be related to several other aspects of core-collapse supernovae [20] including: (i) the compactness of the newly-born proto-neutron star, (ii) the nature of neutrino spectra at decoupling form matter, and (iii) the time between bounce and collapse for progenitors large enough to create black holes [21–24].

5. Results

In order to ensure that the EOS constraints from neutron star observations were robust, several variations were made on the baseline model of the mass and radius constraints from [12]. Four different EOS parameterizations were used, including one which included explicit quark degrees of freedom and one which favored the appearance of phase transitions. The objects with the smallest and largest radius were removed. The largest systematic uncertainty in the interpretation of radii from PRE X-ray bursts is the color correction factor which describes the deviation of the spectrum of the cooling tail from a black body. Different values of the color correction factor were also explored. The final results, from [25], were obtained by choosing the smallest region which enclosed all of the aforementioned variations and are presented in Figure 1. At lower densites, the results are consistent with those obtained from other methods. Note that these constraints now ensure that the maximum mass for all models is large enough to reproduce the recent measurement of a 2 solar mass neutron star [26].

Several oft-used theoretical models are ruled out because they give radii which are larger than the data suggests. From the list of Skyrme models from [27], 1/3 of the models are are ruled out for describing high-density matter [25] (though they may still be appropriate for matter near the nuclear saturation density).

The mass and radius observations also constrain the properties of neutron-rich matter near the saturation density. The first work [29] to clearly connect recent neutron star mass and radius measurements to the symmetry energy at the nuclear saturation density obtained rather low values for the derivative of the nuclear symmetry energy, e.g. 43 MeV $< L <$ 52 MeV in [29] (see Figure 2). This constraint comes, in large part, due to the small radii observed in qLMXBs, especially the neutron stars in M13 and ω Cen. One way around this constraint is to assume a strong phase transition which decreases the pressure in the EOS just above the nuclear saturation density, which raises the constraint to $L <$ 67 MeV [25]. Even this latter weaker constraint rules out some theoretical models which have $L \approx$ 100 MeV. These constraints on L are tighter than most constraints from individual nuclear experiments [30], including those from from nuclear masses ("Masses") [31],

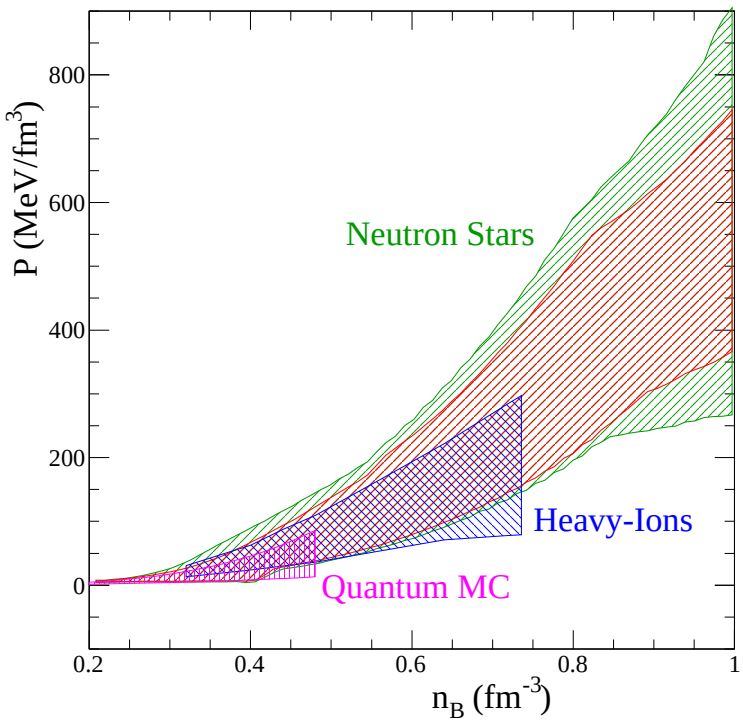

Figure 1: The constraints on the pressure of neutron star matter as a function of baryon number density. The inner and outer regions labeled "Neutron Stars" are the 68% and 95% confidence limits from [25]. The region labeled "Heavy-Ions" is the neutron-matter constraint from [28], corrected for a small number of protons, and the region labeled "Quantum MC" is from [14].

heavy ion collisions ("HIC") [32], pygmy dipole resonances ("PDR") [33], isobaric analog states in nuclei ("IAS") [34], and antiprotonic atoms ("Pb(p,p)") [35].

The aforementioned mass and radius observations have also improved constraints on the radius of a 1.4 solar mass neutron star (Figure 3). Efforts to constraints on neutron star radii have been frustrated by a large number of systematic uncertainties. Not all of these systematic uncertainties are under control. Nevertheless, some of these systematics such as the presence of phase transitions and uncertainties in the spectral shape at in the cooling tails of PRE bursts, can be taken into account by using alternative prior distributions in the Bayesian approach used to analyze the data [25]. Even after having taken these uncertainties into account, neutron star radii more likely lie between 10.4 and 12.9 km (to 95% confidence), a significantly smaller range than the 8 to 15 km suggested earlier. This range of neutron star radii is also consistent with earlier indications from intermediate-energy heavy-ion collisions [36].

The root-mean-square neutron radius in heavy nuclei is strongly correlated with L and also with neutron star radii [37]. The neutron skin thickness, the difference between RMS neutron and proton radii, is thus also constrained by the neutron star mass and radius data. We find that astrophysical data suggest that the neutron skin thickness in lead is relatively small, less than 0.2 fm. This limit is consistent with the current experimental value as obtained in the PREX experiment [38] of $0.33^{+0.16}_{-0.18}$ fm.

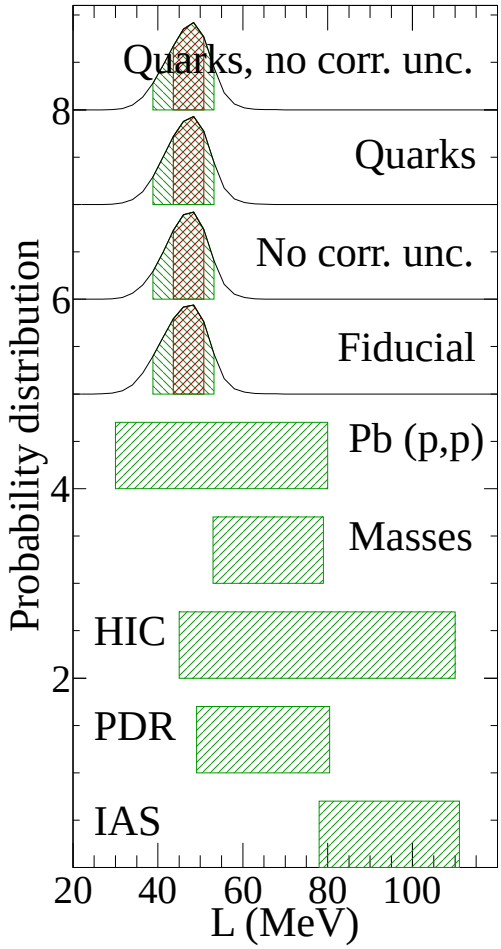

Figure 2: Constraints on the derivative of the symmetry energy energy, L (reprinted from [25] with permission). The top four constraints are from the neutron star mass and radius measurements given different EOS parametrization and assumptions about the symmetry energy, while the five bottom constraints are from analyses of nuclear experiments as described in the text.

The astrophysical observations are also beginning to constrain nuclear three-body forces, in particular the three-neutron force. [14] demonstrated that Monte Carlo simulations using modern nucleon-nucleon interactions were well parametrized by a simple two power-law EOS. A weaker power-law modeling the two-body part of the EOS, and a stronger power-law for the three-body part. [29] showed that the coefficient and exponent of the EOS coming from three-body forces was constrained by the neutron star observations, so long as there was not a strong phase transition just above the nuclear saturation density. In the future, modern three-body forces which would have otherwise been viewed as acceptable, may be ruled out by astrophysical observations.

To construct a supernova EOS table one requires a realistic description of nuclei and nuclear matter over a wide range of densities, temperatures, and electron fractions. Matter below the saturation density at finite temperature consists of a large distribution of nuclei embedded in a background fluid of neutrons, protons, and electrons. However, the gross thermodynamics is well reproduced by a simplified model replacing the nuclear distribution with alpha particles and a single represen-

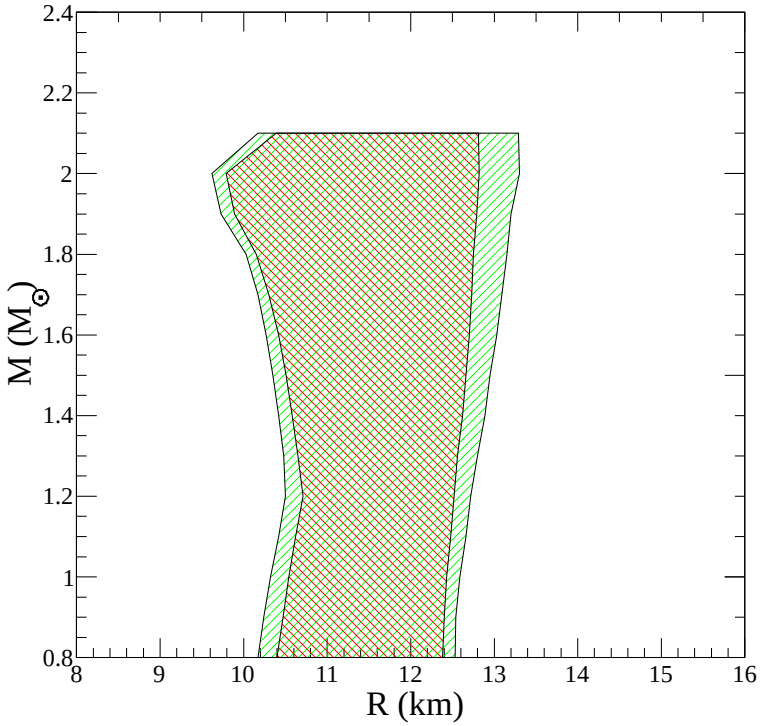

Figure 3: The 68% (green) and 95% (red) confidence limits on radii of neutron stars of a given mass as determined in [25]. Because no observational data is available for larger mass neutron stars, no constraints are obtained for $M > 2.1\ \mathrm{M}_\odot$.

tative heavy nucleus [39]. It is this approximation which was used to create the first supernova EOS tables [40, 41]. Recent works include a larger nuclear distribution and also light nuclei, which are important for describing matter at the neutrinosphere. Ref. [42] has presented several supernova EOS tables with different nuclear interactions and a full nuclear distribution.

Some of these EOS tables, however, are not based on interactions which accurately reproduce the mass versus radius (M−R) curve implied by currently available mass and radius observations. In [24] two new parameterizations of the nucleon interactions were developed by fitting to properties of finite nuclei and the constraints from mass and radius observations. Two new supernova EOS tables, SHFo and SHFx, were then developed from these interactions, by using the model from [43] for the description of nuclei [1]. A summary is given in Figure 4, where several M−R curves from EOS tables are plotted along with the constraints suggested in [12]. Note that these EOS tables for supernovae cannot describe matter out of equilibrium, as is the case for the matter in the crust of an accreting neutron star [44, 45].

6. Future

The most critical requirement for future progress is future observations and future work on disentangling some of the associated systematic uncertainties. It is critical to more carefully under-

[1] Available at http://phys-merger.physik.unibas.ch/∼hempel/eos.html

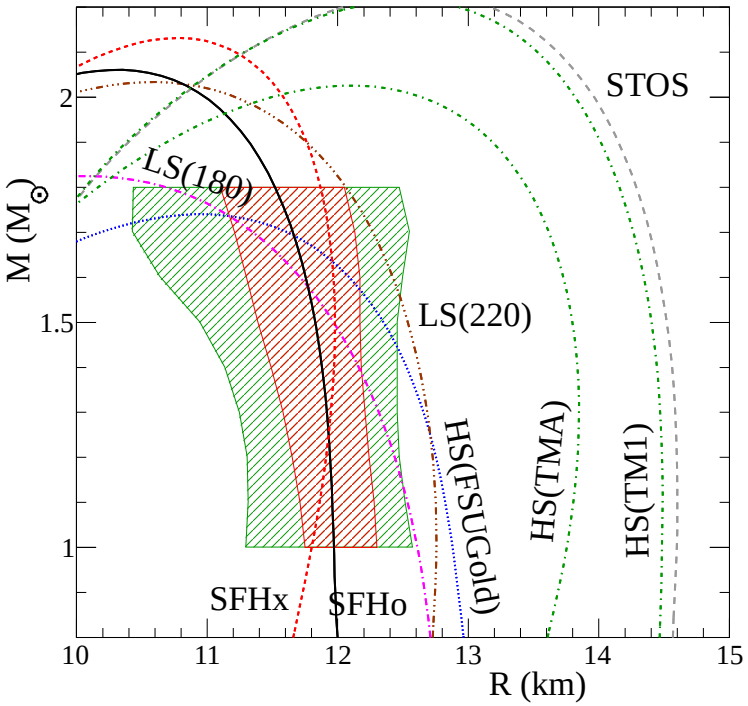

Figure 4: Neutron star mass-radius curve for modern supernova equations of state, adapted from [24]. The red (green) region outlines the one (two) σ confidence limits from [12]. The curves labeled with the "LS" prefix are from [40], the curve labeled "STOS" is from [41], the curves with the "HS" prefix are from [42] and the curves with the "SFH" prefix are from [24].

stand features X-ray spectra: deviation from a black body (e.g. through the color correction factor f_C, spherical asymmetry [46], and the presence of non-thermal emission (e.g. high-energy power-laws [47]). For the PRE burst sources, it is assumed that the Eddington luminosity is achieved at a particular moment in the X-ray burst, and that the shape of the spectrum in the tail of the burst is not changing significantly. Ref [11] has shown that these assumptions may not be correct. It is also still unclear if residual accretion may be playing a role in determining the atmosphere of the quiescent LMXBs.

The work above constrains matter near the nuclear saturation density using astrophysical data, and there is also a separate and large body of work utilizing nuclear data. These analyses need not be separate, and there is a clear opportunity for novel syntheses of astrophysical and nuclear experimental data to generate novel constraints in the future.

7. Acknowledgements

A.W.S. would like to thank E.F. Brown and J.M. Lattimer for several discussions, and is supported DOE Grant No. DE-FG02-00ER41132. T.F. is supported by the Swiss National Science Foundation under project no. PBBSP2-133378. S.G. is supported by DOE Grants No. DE-FC02-07ER41457 (UNEDF and NUCLEI SciDAC) and No. DE-AC52-06NA25396, and by the LANL LDRD program. M.H. acknowledges support from the High Performance and High Productivity

Computing (HP2C) project and the Swiss National Science Foundation (SNF) under project number no. 200020-132816/1. M.H. is also grateful for support from ENSAR/THEXO and CompStar.

References

[1] S. Udry and N. C. Santos, *Ann. Rev. Astron. Astrophys.* **45** (2007) 397.

[2] J. M. Lattimer and M. Prakash, *Phys. Rep.* **442** (2007) 109.

[3] F. Weber, *Pulsars as astrophysical laboratories for nuclear and particle physics*, Bristol, UK, 1999.

[4] C. Y. Cardall, M. Prakash, and J. M. Lattimer, *Astrophys. J.* **554** (2001) 322.

[5] R. Rutledge, L. Bildsten, E. Brown, G. Pavlov, and E. Zavlin, *Astrophys. J.* **514** (1999) 945.

[6] C. O. Heinke, G. B. Rybicki, R. Narayan, and J. E. Grindlay, *Astrophys. J.* **644** (2006) 1090.

[7] N. Webb and D. Barret, *Astrophys. J.* **671** (2007) 727.

[8] J. van Paradijs, *Astrophys. J.* **234** (1979) 609.

[9] F. Ö, T. Guver, and D. Psaltis, *Astrophys. J.* **693** (2009) 1775.

[10] T. Güver, F. Özel, A. Cebrera-Lavers, and P. Wroblewski, *Astrophys. J.* **712** (2010) 964.

[11] V. Suleimanov, J. Poutanen, M. Revnivtsev, and K. Werner, *Astrophys. J.* **742** (2011) 122.

[12] A. W. Steiner, J. M. Lattimer, and E. F. Brown, *Astrophys. J.* **722** (2010) 33.

[13] S. C. Pieper, *AIP Conf. Proc.* **1011** (2008) 143.

[14] S. Gandolfi, J. Carlson, and S. Reddy, *Phys. Rev. C* **85** (2012) 032801.

[15] J. M. Lattimer and M. Prakash, *Astrophys. J.* **550** (2001) 426.

[16] A. Marek and H.-T. Janka, *Astrophys. J.* **694** (2009) 664.

[17] S. Bruenn, A. Mezzacappa, W. Hix, J. Blondin, P. Marronetti, et al., arXiv:1002.4914 (2010).

[18] T. Takiwaki, K. Kotake, and Y. Suwa, *Astrophys. J.* **749** 98 (2012).

[19] B. Müller, H.-T. Janka, and A. Marek, *Astrophys. J.* **756** 84 (2012).

[20] A. Marek, H.-T. Janka, and E. Müller, *Astron. Astrophys.* **496** (2009) 475.

[21] K. Sumiyoshi, S. Yamada, H. Suzuki, and S. Chiba, *Phys. Rev. Lett.* **97** (2006) 091101.

[22] T. Fischer, S. C. Whitehouse, A. Mezzacappa, F.-K. Thielemann, and M. Liebendörfer, *Astron. Astrophys.* **499** (2009) 1.

[23] E. O'Connor and C. D. Ott, *Astrophys. J.* **730** (2011) 70.

[24] A. W. Steiner, M. Hempel, and T. Fischer, arXiv:1207.2184 (2012).

[25] A. W. Steiner, J. M. Lattimer, and E. F. Brown, *Astrophys. J. Lett.* **765** (2012) 5.

[26] P. B. Demorest, T. Pennucci, S. M. Ransom, M. S. E. Roberts, and J. W. T. Hessels, *Nature* **467** (2010) 1081.

[27] J. Rikovska Stone, J. C. Miller, R. Koncewicz, P. D. Stevenson, and M. R. Strayer, *Phys. Rev. C* **68** (2003) 034324.

[28] P. Danielewicz, R. Lacey, and R. Lynch, *Science* **298** (2002) 1592.

[29] A. W. Steiner and S. Gandolfi, *Phys. Rev. Lett.* **108** (2012) 081102.

[30] M. B. Tsang, J. R. Stone, F. Camera, P. Danielewicz, S. Gandolfi, K. Hebeler, C. J. Horowitz, J. Lee, W. G. Lynch, Z. Kohley, et al., *Phys. Rev. C* **86** (2012) 015803.

[31] M. Liu, N. Wang, L. Z.-X., and F.-S. Zhang, *Phys. Rev. C* **82** (2010) 064306.

[32] M. B. Tsang, Y. Zhang, P. Danielewicz, M. Famiano, Z. Li, W. G. Lynch, and A. W. Steiner, *Phys. Rev. Lett.* **102** (2009) 122701.

[33] A. Carbone, G. Colo, A. Bracco, L.-G. Cao, P. F. Bortignon, F. Camera, and O. Wieland, *Phys. Rev. C* **81** (2010) 041301(R).

[34] P. Danielewicz and J. Lee, *Nucl. Phys. A* **818** (2009) 36.

[35] M. Warda, X. Viñas, X. Roca-Maza, and M. Centelles, *Phys. Rev. C* **80** (2009) 024316.

[36] B.-A. Li and A. W. Steiner, *Phys. Lett. B* **642** (2006) 436.

[37] C. J. Horowitz, S. J. Pollock, P. A. Souder, and R. Michaels, *Phys. Rev. C* **63** (2001) 025501.

[38] S. Abrahamyan et al. (PREX Collaboration), *Phys. Rev. Lett.* **108** (2012) 112502.

[39] A. Burrows and J. M. Lattimer, *Astrophys. J.* **285** (1984) 294.

[40] J. M. Lattimer and F. Swesty, *Nucl. Phys. A* **535** (1991) 331.

[41] H. Shen, H. Toki, K. Oyamatsu, and K. Sumiyoshi, *Nucl. Phys. A* **637** (1998) 435.

[42] M. Hempel, T. Fischer, J. Schaffner-Bielich, and M. Liebendörfer, *Astrophys. J.* **748** (2012) 70.

[43] M. Hempel and J. Schaffner-Bielich, *Nucl. Phys. A* **837** (2010) 210.

[44] P. Haensel and J. L. Zdunik, *Astron. & Astrophys.* **227** (1990) 431.

[45] A. W. Steiner, *Phys. Rev. C* **85** (2012) 055804.

[46] M. Zamfir, A. Cumming, and D. K. Galloway, *Astrophys. J.* **749** 69 (2012).

[47] S. Guillot, M. Servillat, N. A. Webb, and R. E. Rutledge, arXiv.org:1302.0023 (2013).